Library Progress International
Vol.44 No.3, Jul-Dec 2024: P.5407-5425

Print version ISSN 0970 1052
Online version ISSN 2320 317X

Original Article

Available online at www.bpasjournals.com

Deciphering and Validation of Urbanization of Metropolitan Region in South Asia using Urban Night Lights (UNL): A Case Study of Kolkata Metropolitan Area (KMA), West Bengal, India

***Abhinandan Das**

*Department of Humanities and Social Sciences, Indian Institute of Technology, Kharagpur 721302, West Bengal, India. abhinandandas24@gmail.com

How to cite this article: Abhinandan Das (2024) Deciphering and Validation of Urbanization of Metropolitan Region in South Asia using Urban Night Lights (UNL): A Case Study of Kolkata Metropolitan Area (KMA), West Bengal, India. *Library Progress International,* 44(3), 5407-5425

Abstract

Images of brightness in the darkness of night obtained from satellite images are considered evidence of the location and expansion of urban areas. The location of electrification in urban areas dramatically increases the night sky's brightness. The urban expansion of the KMA region from 2001 to the present 2021 has been very high and has had a significant impact on the region's environment and people. In this article, the urban expansion of the KMA region since 2001 has been highlighted through images of urban night lights (UNL) based on decades, and urban expansion has been validated by comparing it with various temperate spatial indices. Through observation, it has been seen that with the increase in the built-up area between 2001 and 2021, the amount of LST and NDBI has increased, and the amount of luminous value of UNL has increased significantly. At the same time, NDVI or MNDWI decreased substantially with the increase in luminous value, which proves urban expansion through deforestation and wetland encroachment.

Keyword: Urban Night Light, Luminous Value; LST; NDBI; MNDWI; NDVI

Introduction

From the dawn of civilization to the present, as urban areas expand with the increase in population, pollution increases due to changes in land use and climate. Due to the gradual change of global population and the restriction to a specific urban area due to various amenities, the area gradually changes, and finally, the UHI (Urban Heat Island) originates. The UHI concept analyses the aspects of urban regions' expansion and climate change (Li & Zhou, 2017). In the present era, a wide range of contemporary technologies and materials are employed globally to comprehend the growth of metropolitan regions. Primarily, these technologies assess the effects of human-modified land use on ecosystems and the environment in metropolitan areas. Satellite data is used to analyse the expansion of an urban region and evaluate its qualitative and quantitative characteristics over different decades. This information allows us to determine the rate of future changes. In the early 21st century, we recognised that the cyclical transformations of a vast urban region can only be witnessed from outer space (Zheng et al., 2023; Rehman et al., 2022; Katabaro et al., 2022). Urban night illumination assessment is a crucial indicator of how much humans have affected the Earth's surface. It is advantageous for discerning human settlements and business endeavours. The objective of the UNL (Urban Night Lighting) project is to assess the practicality of consistently observing and monitoring human activities, as well as understanding and analysing their environmental impacts (Satheendran et al., 2022; Liao et al., 2023; Li et al., 2023). The assessment will evaluate the advantages of utilising optical, infrared, luminous, and radar satellite products to monitor human activities. Global night-time lights are widely recognised satellite data products that graphically depict human activity on the Earth's surface and the growing pace of urbanisation. In addition, researchers from other disciplines, such as economists, biologists, and astronomers, utilise the global categorisation of illuminated areas and their corresponding levels of brightness (Defries et al., 2022; Ma et al., 2012; Bhandari & Roychowdhury, 2011). The generation of worldwide night-time illumination requires a significant number of observations during the night, especially those of exceptional quality, and sophisticated electronics to consistently measure brightness as seen from space. UNL

is currently the most advanced technique used in the world to analyze the periodic expansion of urban areas over time. However, the UHI concept is explored through land use change, i.e. LULC analysis and its surrounding climatic changes from LST, NDVI and MNDWI data obtained from satellite images, which gradually reveal various aspects of temperature, vegetation and wetland changes with the UHI concept (Bagan et al., 2019; Cheon & Kim, 2020; Gilbert & Shi, 2023). The periodic changes in UHI and the increase in building volume are also reflected in NDBI. However, the UNL concept's current use helps validate the periodic changes in the UHI. Because all the buildings in urban areas are electrified, they are easily captured in satellite images at night, proving the direction of metropolitan areas' expansion.

Reducing greenery due to construction in a particular area gradually introduced the UHI concept (Nieuwolt, 1966). The continuous change of LULC over time makes the issue of UHI more significant (Neteler, 2010). The UHI phenomenon is affected by many patterns of LULC alteration, which include modifications in vegetative cover levels, agricultural areas, and urban expansion due to factors such as building materials, spacing of homes, road construction, and the presence of railway stations. The magnitude and extent of the UHI are assessed by assessing the LST and the emissivity ratio at ground level. Sunlight is reflected directly from the ground and travels up the atmosphere as long waves radiate into the dome shape of the UHI and cause the LST. LST also changes with the change of LULC (Pramanik & Punia, 2019; Fitrahanjani et al., 2021). The phenomenon known as the UHI effect was attributed to the expansion of the urban area in conjunction with LST. LULC change in a region is mainly accelerated by dense urban construction, as emphasised by Verma et al. (2020). LST oscillates significantly due to land-use changes driven by different metropolitan area growth plans (Stemn & Kumi-Boateng, 2020). While measuring surface temperature is tricky, measuring LST through satellite image bands is much easier. In UHI context, LST is utilised to classify land use through images. The data is obtained from spaceborne information's thermal infrared remote sensing (TIR) divisions. The shifting of urban heat island (UHI) patterns over time within a particular urban area indicates both climatic change and land-use alterations (Jain et al., 2020). The alteration in land use and land cover (LULC) directly impacts the quantity of land surface temperature (LST), therefore influencing the positioning of the urban heat island (UHI). There is an inverse relationship between the number of green plants in a region and the temperature, meaning that many green plants result in a very low temperature. In addition to NDVI, the existence of water also plays a role in determining the temperature of a location. The position of UHI is subject to significant variation due to NDVI, as stated by Asgher et al. (2021). In Southeast Asian nations, such as India, the summer season significantly increases temperatures, whereas locations close to bodies of water experience comparatively lower temperatures. However, analysing the patterns of land use reveals a significant rise in land surface temperature (LST) in areas designated for human habitation. Studies undertaken by Gupta et al. (2019) and Bera et al. (2021) have shown that temperatures near water bodies are often lower than those in more distant places. Also, the expansion effect of UHI is well seen in the amount of wetland and building area. The extent of wetlands in any urban area is derived through MNDWI analysis. Generally, when the urban area expands, the number of wetlands decreases because the urban area expands by burning the wetlands. Again, as the number of buildings increases, the urban area expands, and the LST, as measured by the NDBI, increases. However, the best UNL method in the world can calibrate and validate qualitative and quantitative analysis of UHI. UNL is calculated by extracting the DN value of the luminous region of the nighttime satellite image. This analysis shows that UNL has a positive proportional relationship with LST and NDBI and a negative exponential relationship with NDVI and MNDWI. Satellites such as NASA's Landsat series, SPOT, Quick Bird, World View, IKONOS, and Maxar of France take pictures of night conditions, but they could be better and are much more expensive, which are beyond the reach of the general public (Yi et al., 2014; Zhao et al., 2028; Satheendran et al., 2022). However, in comparison, the nighttime data captured by the Defence Meteorological Satellite Program's Operational Line Scan System (DMSP/OLS) is much more cost-effective and accurate and is easily within the needs of the general public. The data obtained from DMSP/OLS can easily distinguish rural from urban areas and highlight urban regions' spatial and temporal variation. The DMSP/OLS satellite's ability to detect lower light levels, accurately quantify them, provide higher resolution photos, and calibrate in-flight distinguishes it from previous satellite imaging systems (Satheendran et al., 2022; Li et al., 2023).

In 1965, West Bengal Act XIV and in 1979, West Bengal Act XIII Greater Kolkata or KMA (Kolkata Metropolitan Area) came into being, and its autonomy rests on KMDA (Kolkata Metropolitan Development Authority). Consisting of 4 Municipal Corporations and 37 Subsidiaries in five districts, the KMA region has a total area of 1,888 km^2 and a total population of 15,870,000. In terms of area, this region ranks 13th in Asia and

16th in the world, but it ranks third in India. The KMA area is detailed: Chandannagar Municipal Corporation in the north, Sonarpur-Rajpur Municipality in the south, Kalyani and Haringhata Municipalities in the northeast, and Uluberia Municipality in the southwest. Since 2001, the urban expansion of the region has been going through gradual changes and the region's population is expected to increase by 2.5 times in 2021. As the temperature of the KMA region has increased with the continuous growth of urban areas, wetlands and greenery have also changed the land use. This paper aims to evaluate the efficacy and significance of UNL remote sensing data in understanding urbanisation patterns from 2001 to 2021. Furthermore, it examines the connection between UNL and LULC changes over time and their association with other spatial climatic and ecological parameters. The goal is to get a deep understanding of the complex dynamics that influence the process of urbanisation and changes in the ecology within the KMA region. The validation of changes in urban expansion with meteorological and ecological parameters over 30 years primarily relies on UNL data collected through patch-based satellite imagery analysis. This study aims to fill a scientific gap by conducting extensive studies correlating UNL data with urban growth. Specifically, the study examines the relationship between climate and ecological changes by analysing the association between Landsat results and changes in several metrics.

2 Materials and methods

2.1 Study area

Kolkata, the capital of West Bengal in India, was originally established by the British. It is situated in a flat region with tide-dominated drainage outfalls. The Kolkata Metropolitan Area (KMA), which includes the city of Kolkata, is one of the world's most important urban areas. KMA, known as The Kolkata Urban Agglomeration (KUA), has experienced consistent growth throughout the past century. KUA spans an area of around 1851 square kilomerters and is situated between latitudes 22˚ 0’19’’and 23˚0’01’’ in the north and 88˚0’04’’ and 88˚ 0’33’’ in the east (Fig 1). The Hooghly River is a vital lifeline for the entire Southern Bengal region. The city of Kolkata, with its urban sprawl, is situated along both the eastern and western banks of the river, forming a linear urban layout. The rural hinterland envelops the urban area, serving as a buffering green belt around the agglomeration (KMC 2015). This intricate network of local governments in South Bengal includes 38 towns, 77 census towns (CT), 16 expansions, 445 rural villages, and three large municipal corporations (MC): Kolkata, Howrah, and Chandernagore.

With a density of 7950 people per square kilometre, the 2011 Census put the total population of the KMA at approximately 14.72 million. With a projected yearly growth rate of 1.8%, the Indian population is expected to reach 20 million in 2021 and 21.1% in 2025, according to the 2011 Census of India and the KMDA. With a combined population of almost 30 million, the megacities that make up the Kolkata metropolitan agglomeration are among the most populous in the world (UN, 2007). Among India's urban agglomerations, Kolkata ranks third in size. As it grows into a major metropolis, perhaps in comparison to other cities worldwide, Kolkata faces several socioeconomic challenges, including heavy traffic, poverty, overcrowding, noise, water, and air pollution (Bhatta, 2009; Mukherjee, 2012).

On top of that, 33 per cent of the people living in the slums of KMA are poor. Multiple land uses, including residential, commercial, and industrial, coexist in the metropolitan agglomeration's slums (Roy et al., 2014). Swamps and marshy areas abound in the easternmost part of the KMA, especially in Bidhan Nagar, Rajarhat, Maheshtala, and Sonarpur. Without adequate planning, these wetland areas are transformed into urban areas by constructing homes (Dasgupta et al., 2013).

According to LULC, based on three decades of the KMA region, all LULC are divided into eight categories (Fig 3). The total agricultural land in 2001 was 513.24 sq km, which has become 431.23 in 2011 and 290.46 sq km in 2021. Therefore, from 2001 to 2021, agricultural land has decreased by 12.46%. In 2001, the extent of bare land in the KMA region was 61.77 sq km, which increased to 87.37 sq km in 2011. However, in 2021, the amount of bare land was reduced to 38.97 sq km, and from 2001 to 2021, the amount of bare land decreased by about 1.28%. The urban construction or built-up area was 319.51 sq km in 2001, gradually increasing to 411.35 sq km in 2011 and 543.91 sq km in 2021. The built-up area in the KMA region increased by 12.55% in the three decades from 2001 to 2021. In 2001, the amount of fallow land was 23.26 sq km, and in 2011, it increased to 40.13 sq km. In 2021, the amount of fallow land decreased significantly to 23.32 sq km, and the rate of increase or decrease of fallow land remained unchanged from 2001 to 2021. In 2001, the extent of the homestead was 184.79 sq km, and in 2011, it increased to 379.09 sq km. In 2021, this amount decreased to 262.24 sq km; from 2001 to 2021, homestead increased by 4.33%. In 2001, the forest area in the KMA region was 530.91 sq km,

and in 2011, it decreased to 262.56 sq km. In 2021, people increased the amount of forest area for their own needs by 452.6 sq km, and the rate of forest loss from 2001 to 2021 is 4.38%. The size of the water body was 92.04 sq km in 2001 and increased to 116.79 sq km in 2011. In 2021, the extent of the waterbody decreased slightly to 109.21 sq km, and from 2001 to 2021, the extent of the waterbody increased roughly by 0.96%. In 2001, the extent of the wetland was 61.85 sq km, and in 2011, the extent of the wetland decreased slightly to 58.87 sq km. Later, in 2021, the wetland increased to 66.68 sq km, and the growth rate of wetlands from 2001 to 2021 was about 0.27% (Fig 4).

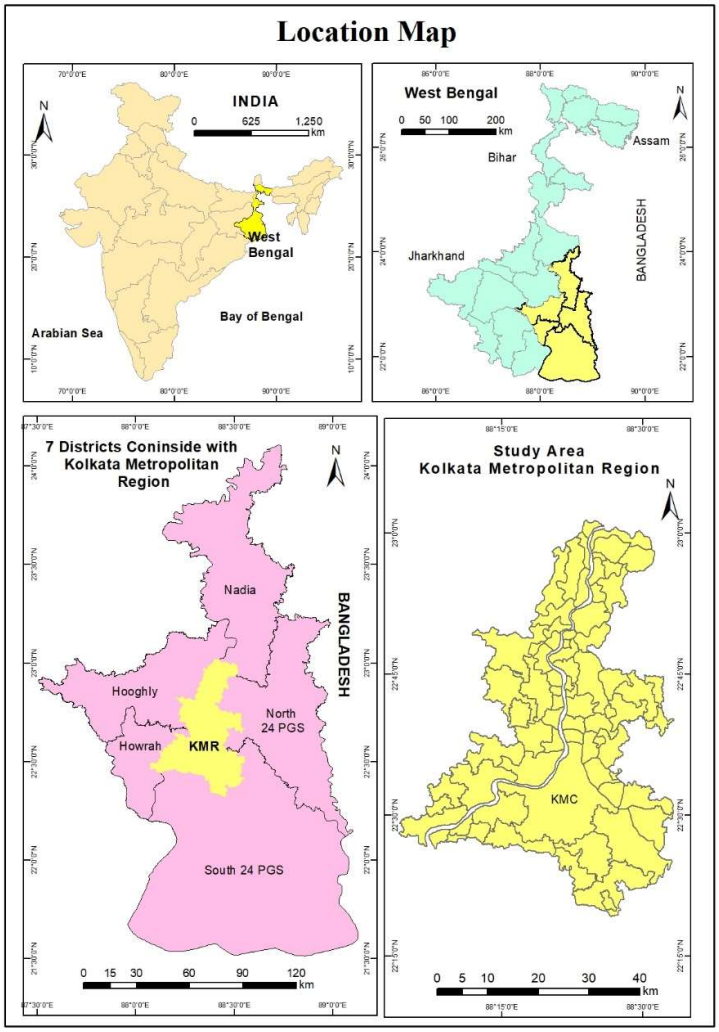

Fig. 1 Location of KMA area

2.2 Data used

2001 and 2011 LANDSAT 5 TM and 2021 LANDSAT 8 OLI satellite images were collected from Earth Explorer for LULC, NDVI, MNDWI, NDBI and LST analysis of KMA area. Their accuracy has been determined in a planned way by fixing the images based on specific coordinate systems and projections. Also, several errors in the images collected from Earth Explorer have been corrected and analysed according to mathematical and radiometric methods. Also, images without clouds were collected between November and March. We did all the work through QGis and Erdas Imagine. Except that, DMSP/OLS images from 2001 to 2021 is gathered with the gap of 10 years to validate the UHI process of KMA region.

2.3 Methodology

2.3.1 Extraction of Land use land cover

The Landsat 5 TM satellite was utilised to capture images in 2001 and 2011, while the Landsat 8 OLI satellite was employed to capture the images in 2021. The picture classification task utilised the Support Vector Machine

(SVM) supervised classification method, resulting in the extraction of six primary LULC classes (Hu et al., 2018). The LULC classifications are obtained by categorising land into agricultural, barren, built-up areas, vegetation, water bodies, fallow land, homestead and wetlands. A validation process is carried out by digitising 400 samples from GEE to assess the accuracy of the selected LULC classes (Jia et al., 2019). The reference data is used to construct a confusion matrix. The error matrix was employed to evaluate the overall accuracy and the Kappa coefficient.

2.3.2 Analysing accuracy of LULC

The primary purpose of determining the accuracy of a satellite image is to determine how similar it is to the terrain. In the case of LULC, the accuracy of the satellite image is enhanced by how we classify it through the supervised image. An image's accuracy can be evaluated through,

$$\text{Overall Accuracy} = \text{Total number of correct samples} * 100\% \text{ total number of samples} \quad (1)$$

The authenticity of every distinction and category is determined within this investigation using a uniform formula. Zhou et al. (1998) and Lunetta et al. (2001) assert that a user's precision can be evaluated by examining metrics related to commission mistakes. The Kappa Coefficient is the primary metric for assessing accuracy (Ma & Redmond, 1995). The accuracy of three land use analyses has been assessed in this study using the Kappa coefficient. Take the detection stage (N) as an example and divide it by the diagonal frequency (∑a). After that, it speeds up at the total expected frequency (ef), split by removing all standard frequency (ef) overviews from 1. Kappa can take on values between 0 and 1, with 0 indicating a decrease in perfection and 1 representing an absolute truth. This Kappa's value is far below 0.40, indicating a lower level of accuracy in the proposal. On the other hand, according to Monserud & Leemans (1992), it is considered fair when the value is between 0.40 and 0.55, expensive when the cost is between 0.55 and 0.70, and best explained when the amount is between 0.70 and 0.85. The procedure is,

$$K = \frac{\frac{\Sigma a}{n} - \sum ef}{1 - \sum ef} \quad (2)$$

$$\text{Expected Frequency (ef)} = \text{row total} * \text{column total/N} \quad (3)$$

Using a change matrix, we are analyzing the alterations in LULC photographs spanning from 2001 to 2021, with a time interval of ten years (Weng, 2001). The calculations of land-use changes' gain and loss have been determined through this process.

2.3.3 Compute LST

Thermal infrared data obtained from Landsat satellite images with a spatial resolution of 100 to 120 m helps to provide information on LST (Qin et al., 2001). According to scientists, LST is determined from the infrared radiation emitted by the earth in the thermal band spectral range of 10.4 to 12.5 µm as long waves (Liu & Zhang, 2011). Three main steps typically calculate LST. First, the conversion of the digital number to spectral radiance (Lλ) can be done using the equation provided by the Landsat Project Science Office in 2002. Additionally, a new form is available for this conversion.

$$L(\lambda) = \text{gain} * DN + \text{offset} \quad (4)$$

$$L(\lambda) = \frac{LMAX - LMIN}{255} * DN + LMI \quad (5)$$

Whereas L(λ) represents the spectral radiance in W.m-2.sr-1.m-3, LMIN (1.32) and LMAX (13.67) correspond to the spectral radiance of band 6 with a DN value of 0 and 255, respectively. Furthermore, apply the methods suggested by Artis and Carnaham in 1982 to transform the spectral radiance into temperature measured in Kelvin.

$$TB = K_2/In(\frac{K_1}{L\lambda} + 1) \quad (6)$$

TB represents the brightness temperature measured by satellites, specifically LANDSAT 8 OLI and LANDSAT

TM. K_1 and K_2 are calibration constants unique to these satellites' distinct bands. Finally, the conversion from kelvin to Celsius is accomplished using the following formula,

$$TB = TB - 273.15 \quad (7)$$

The equation used to determine the Land Surface Temperature (LST) for Landsat 5 TM is as follows,

$$T_s = 1/C\,[\alpha(1 - C - D) + (b(1 - C - D) + C + D)\,BT - DT_a] \quad (8)$$

Where T_s represents LST, ε denotes emissivity, and τ refers to total atmospheric emissivity. The equation for mean atmospheric temperature is T_a=17.9769+0.9171T_0. The variables C and D are calculated using the values of ε and τ. ε is equal to 0.99 and τ is equal to 0.9. The constants α and b are adopted from Qin et al. 2001 and have values of -67.355351 and 0.458606, respectively. T_0 represents the temperature of the air near the surface. For Landsat 8 OLI, the equation used to determine the LST is as follows:

$$T_s = \frac{BT}{1 + [(\frac{\lambda BT}{\rho}) \ln \varepsilon\lambda]} \quad (9)$$

In the equation, the emitted radiance wavelength is denoted by λ, while ρ equals h (C/σ) (1.438*10-2mK). The Boltzmann constant is represented by σ, Planck's constant by h, and the velocity of light by C.

2.3.4 Calculate emissivity values

Accurate adjustment of spectral emissivity is essential for calculating LST in all geographical areas (Snyder et al., 1998). Calculations entail deriving emissivity values from NDVI measurements for every pixel. Upon implementing the required modifications, the formula now displays in the following manner,

$$\text{Land Surface Emissivity } (€) = 0.004 * Pv + 0.986 \quad (10)$$

Calculating the proportion of vegetation (Pv) in this area involves

$$Pv = \{(NDVI - NDVI_{min})/(NDVI_{max} - NDVI_{min})\}^2 \quad (11)$$

2.3.5 Spatial structure of LST

The exclusion of the wetland component from the water causes a noticeable change in the slope of each LST profile during interpolation (Gupta et al., 2019). Regarding interpolation, the weighted average is computed based on the proximity of each adjacent point. The remaining data are consolidated by integrating them, utilizing the average as the foundation. The weighted average and linear function (x_1, y_1 and x_2, y_2) are computed using data from two distinct points (Gupta et al., 2019).

$$Y = \frac{x_2 - x}{x_2 - x_1} + \frac{x - x_1}{x_2 - x_1} y_2 \quad (12)$$

$$L(X) = \frac{x_2 - x}{x_2 - x_1} + \frac{x - x_1}{x_2 - x_1} y_2 \quad (13)$$

2.3.6 Compute relation between LST and NDVI, MNDWI and NDBI

The NDVI has been computed utilizing Landsat data to illustrate the relationship between surface temperature, area coverage, hydrological systems, and vegetation abundance. The computation of NDVI is performed using the approach described by Townshend and Justice in 1986.

$$NDVI = \frac{\text{NIR band} - \text{R band}}{\text{NIR band} + \text{R band}} \quad (14)$$

NIR is an abbreviation for the near-infrared wavelength range, whereas R denotes the red wavelength range. The computation of NDVI has been conducted utilising bands 3 and 4 for LANDSAT TM data and bands 4 and 5 for LANDSAT OLI data. NDVI is employed to signify the existence of plant life in a particular geographical area. MNDWI is calculated by,

$$MNDWI = \frac{\text{Green band} - \text{SWIR band}}{\text{Green Band} + \text{SWIR band}} \quad (15)$$

Where Green means green band, and SWIR is the short wave-infrared band. For LANDSAT TM data, band 3 and 5 and for LANDSAT OLI data band 3 and 6 have been used to compute MNDWI. MNDWI is utilized to signify the water indicator of an area. NDBI is derived by (Zha et al., 2003),

$$\text{NDBI} = \frac{\text{MIR band} - \text{NIR band}}{\text{MIR band} + \text{NIR band}} \quad (16)$$

Where MIR is the middle infrared band, and NIR is the near-infrared band. For LANDSAT TM data, band 5 and 4 and for LANDSAT OLI data band 6 and 5 were used to calculate NDBI.

2.3.7 Compute UNL data and validate with previous indices

The UNL data offers essential insights into urban growth and human activities. The DMSP-OLS dataset provides spatially resolved night-time light data at 1 km by 1 km from 2001 to 2021. These databases record artificial lighting at night, which makes it possible to evaluate patterns of urbanisation, regional economic activity, and population distribution. They are extensively employed in many domains, such as socioeconomic research, urban planning, and environmental monitoring. They offer a potent resource for researching the effects of humans on the environment and monitoring alterations in patterns of night-time light throughout time. Published studies (Duque et al., 2019; Levin et al., 2020; Zheng et al., 2023; Xin, 2023) have shown a high correlation between night-time light statistics, population density, and area economic activity. This study used UNL data from 2001, 2011, and 2021 to investigate the relationship between urban development and expansion.

Consequently, this was achieved by integrating geographical data, which enabled us to graphically illustrate the connection between UNL patterns and the expansion of urban areas during the designated periods. Compared to DMSP-OLS, the Visible Infrared Imaging Radiometer Suite (VIIRS) of the day/night band (DNB) provides Night-Time Light (NTL) data, which is highly helpful in mapping precise borders worldwide with a more excellent spatial resolution. The VIIRS's NTL data exhibits a stronger positive correlation with social interactions, providing insight into the underlying causes of cities' emergence and growth.

3 Results and discussions

3.1 Changes in LULC (2001-2021)

Three decades of LULC change in KMA region are highlighted by analysing satellite images obtained every 10-year interval from 2001 to 2021. The overall accuracy of satellite images from 2001 to 2021 is 87.21%, 88.93% and 90.23%, respectively. The kappa coefficient value also changed depending on this accuracy: 0.784, 0.729, and 0.846.

According to satellite images from 2001 (Fig 2), the land use of the entire KMA region is primarily agricultural land along Baruipur, Budge Budge, Jaynagar Majilpur, Maheshtala, Pujali, Rajpur Sonarpur in the South and South East. Also, there is a large amount of agricultural land in Baidyabati, Bhadreswar, Champdani, Dankuni, and Hugli Chuchura regions in the west and along Haringhata, Kalyani in the north. The influence of urbanization and the presence of built-up areas can be seen in the areas on both banks of the Hooghly River, including the Kolkata region in the middle. Mainly due to the convenience of the communication system and proximity to Calcutta, the population here is very high. Many water bodies and wetlands can be seen in the southeast of the KMA region near Salt Lake, Rajarhat and Bidhannagar. Also, waterbodies and wetlands can be seen in various parts of Hooghly and South 24 Parganas districts under KMA. The extent of greening is limited to central and northern Hooghly, Nadia and North 24 Parganas districts, excluding urban areas. Fallen land can be seen in some parts of Kalyani, Dankuni, Uttarpara-Kotrang municipality and Chandannagar Municipal Corporation. Fallow land can be seen in some parts of Kanchrapara, Bhatpara, Chandannagar, Bally, Dankuni and Bidhannagar.

According to the 2011 LULC (Fig 2), agricultural land has decreased across the southeast regions of Jaynagar Majilpur, Maheshtala, Pujali, and Rajpur Sonarpur. Again, in the southwest, towards Bajbaj and Uluberia, the amount of greenery has decreased, and agricultural land has taken over that area. Along both sides of the Hooghly River till Kalyani in the north, the amount of greenery has reduced, and the amount of agricultural land has increased, indicating human activity and food supply. Madhyamgram, Naihati, New Barrackpore, North Barrackpur, North Dumdum, Panihati, South Dumdum, Titagarh, etc., along the eastern side of the KMA region, the amount of urban construction has increased a lot. Also, urbanization in Uluberia in the southwest has increased significantly. In Hooghly district, building construction has increased from Vaidyabati to Konnagar to Dankuni. Along with this, the amount of greening and forestry has dramatically decreased. It has become agricultural land or urban construction by cutting down the forest. Although the amount of waterbody has increased, the amount of wetland has reduced slightly. Although the number of water bodies is the same near Salt Lake and Rajarhat in the South and South East, the number of wetlands has increased somewhat between Konnagar to Chandannagar and Barrackpore to Naihati. The amount of fallow land near Rajarhat was the same in the past, but the amount between Dankuni and Vaidyabati increased quite a bit. The bare land on both sides of the Hooghly River along the middle section has increased considerably.

considerably.

At present, i.e. in 2021 (Fig 2), the amount of agricultural land has decreased a lot. Agricultural lands are concentrated in Kalyani, Haringhata in the north, some areas in the middle and Rajpur-Sonarpur region in the south. The amount of bare land has decreased a lot, and urban construction has increased excessively. Most bare and fallow land has gradually been turned into urban construction. Although the amount of vegetation decreased in 2011, people have increased it by making gardens that are planned for their own needs. Compared to 2011, the amount of water bodies has decreased, but people have created several wetlands for their needs. Most of the wetl According to LULC, based on three decades of the KMA region, all LULC are divided into eight categories (Fig 3). The total agricultural land in 2001 was 513.24 sq km, which has become 431.23 in 2011 and 290.46 sq km in 2021. Therefore, from 2001 to 2021, agricultural land has decreased by 12.46%. In 2001, the extent of bare land in the KMA region was 61.77 sq km, which increased to 87.37 sq km in 2011. However, in 2021, the amount of bare land was reduced to 38.97 sq km, and from 2001 to 2021, the amount of bare land decreased by about 1.28%. The urban construction or built-up area was 319.51 sq km in 2001, gradually increasing to 411.35 sq km in 2011 and 543.91 sq km in 2021. The built-up area in the KMA region increased by 12.55% in the three decades from 2001 to 2021. In 2001, the amount of fallow land was 23.26 sq km, and in 2011, it increased to 40.13 sq km. In 2021, the amount of fallow land decreased significantly to 23.32 sq km, and the rate of increase or decrease of fallow land remained unchanged from 2001 to 2021. In 2001, the extent of the homestead was 184.79 sq km, and in 2011, it increased to 379.09 sq km. In 2021, this amount decreased to 262.24 sq km; from 2001 to 2021, homestead increased by 4.33%. In 2001, the forest area in the KMA region was 530.91 sq km, and in 2011, it decreased to 262.56 sq km. In 2021, people increased the amount of forest area for their own needs by 452.6 sq km, and the rate of forest loss from 2001 to 2021 is 4.38%. The size of the water body was 92.04 sq km in 2001 and increased to 116.79 sq km in 2011. In 2021, the extent of the waterbody decreased slightly to 109.21 sq km, and from 2001 to 2021, the extent of the waterbody increased roughly by 0.96%. In 2001, the extent of the wetland was 61.85 sq km, and in 2011, the extent of the wetland decreased slightly to 58.87 sq km. Later, in 2021, the

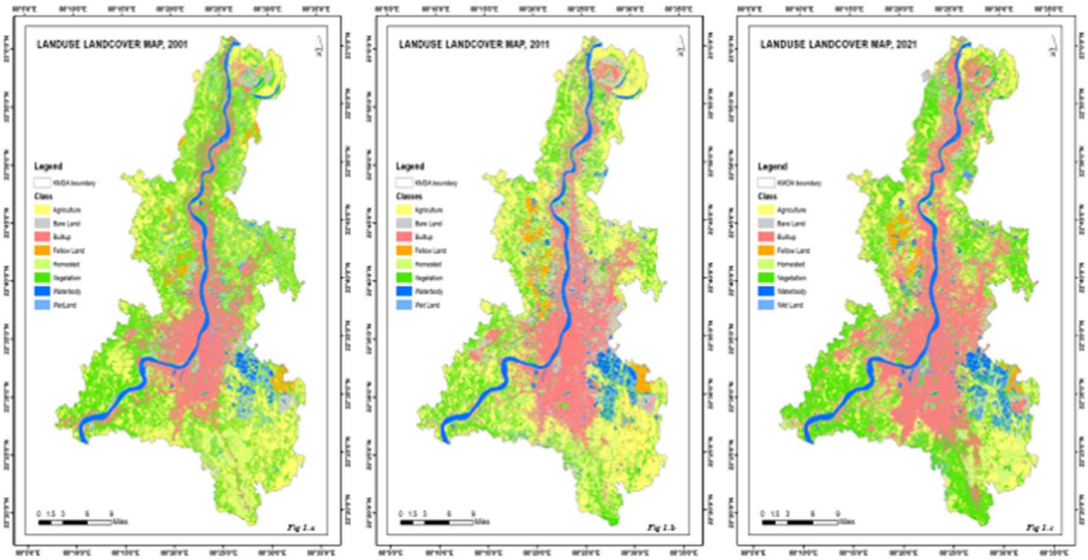

wetland increased to 66.68 sq km, and the growth rate of wetlands from 2001 to 2021 was about 0.27% (Fig 4).ands have been developed as fish ponds

Fig. 2 LULC map of KMA region from 2001 to 2021

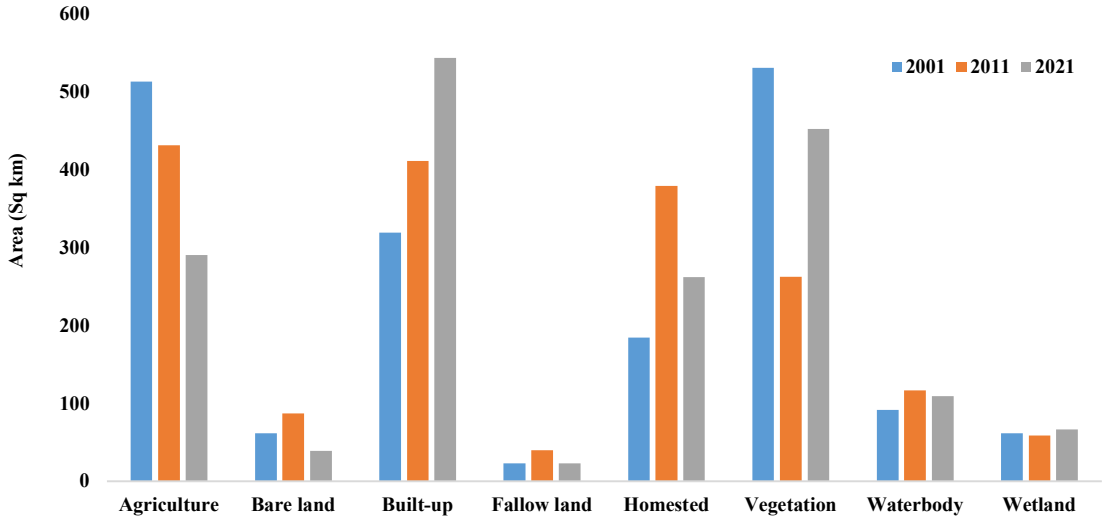

Fig. 3 Different LULC classes with their changing amount from 2001 to 2021

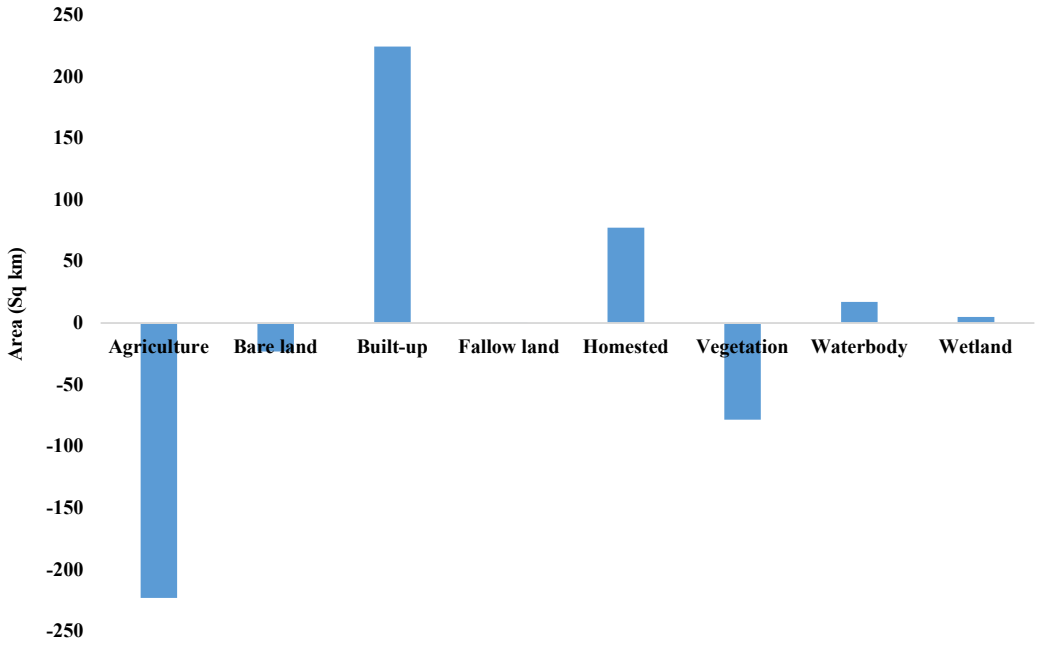

Fig. 4 Areal differentiation on LULC classes in KMA area

3.2 Changes in NDVI (2001-2021)

The density sliced pictures for the years 2001, 2011, and 2021 are displayed in Figure 5. As can be observed, compared to 2001, the non-vegetated area has significantly risen in the 2011 photograph. The built-up region increasingly extends beyond the city's boundaries, particularly on the eastern and southern sides. Figure 5 depicts the city core (Kolkata and the surrounding regions) in 2001 with moderately low to moderate vegetation. By 2011, however, this vegetation had shifted to moderately low levels, and by 2021, most of it had become a moderately highly vegetated area. This is because, formerly, this area was covered with sparse vegetation and natural bushes, but with an increase in population, new residential complexes have been built here. Furthermore, because the city is a metropolis and urbanization are proliferating, the vegetation cover was relatively low in 2011. Still, this vegetation cover rose due to a lockdown scenario in 2021. Similar to the Madhyamgram-Barasat region in Figure 5, located in the city's eastern portion, this area was formerly an agricultural one. Still, the city's growing population has turned the whole territory into a built-up area. The Sankrail region follows a pattern in which

moderate to thick vegetation has reduced between 2001 and 2011 and grown between 2011 and 2021.

Fig. 5 Areal differentiation in NDVI of KMA area from 2001 to 2021**3.3 Changes in LST (2001-2021)**

The land surface temperature (LST) was determined using the mathematical approach in different previous

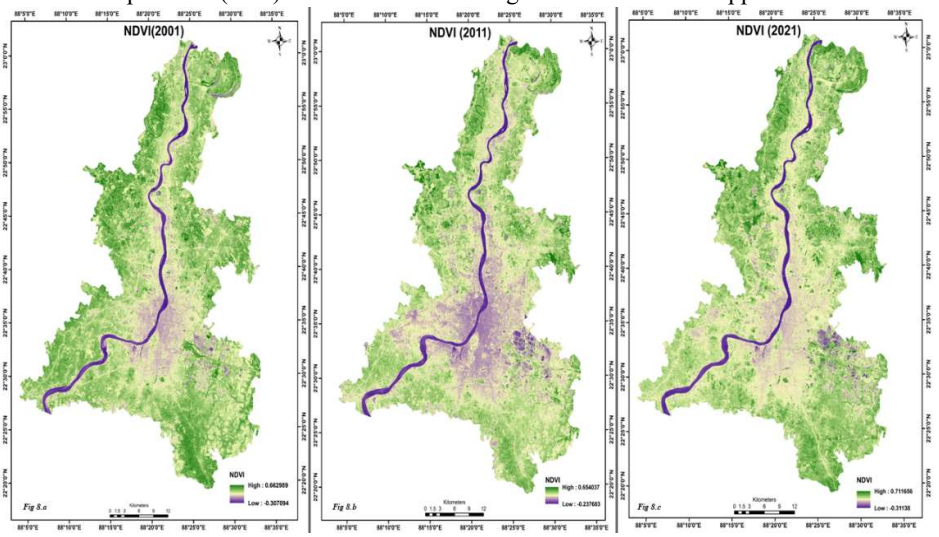

equations. According to Landsat data, the mean estimated dry bulb temperature for KMA in 2001, 2011, and 2021 was 25.8°C, 29.9°C, and 31.6°C, respectively. Figure 6 displays the value of the LST of each class for the years 2001, 2011, and 2021 at the micro-level of the analysis. In 2001, thick vegetation (17.4°C) and open space (17.9°C). The study found that surface temperature decreased as it moved towards the outer boundaries, which was related to the different land use patterns. Based on the investigations, the waterbody had an average surface temperature of 17.01°C and demonstrated a significant capability for heat retention and transportation. The city's central section, where most of the built-up area was located, recorded the highest temperature of 23.25°C. In 2001, 14.25°C was the lowest surface temperature recorded, while 25.83°C was the highest.

According to the visual depiction and LST data for each land use class in 2011, the surface temperature for the low temperate zone was 14.71°C to 19.8°C. The average surface temperature for the mild temperate zone ranged from 19.8°C to 24.9°C. The central part of KMC has the most significant temperature zone (24.9°C-30°C) recorded. However, the LST value was also reported at 30°C in several isolated areas/locations. The lowest and greatest surface temperature values in 2011 were 14.7°C and 30°C, respectively. According to Figure 6, the lowest

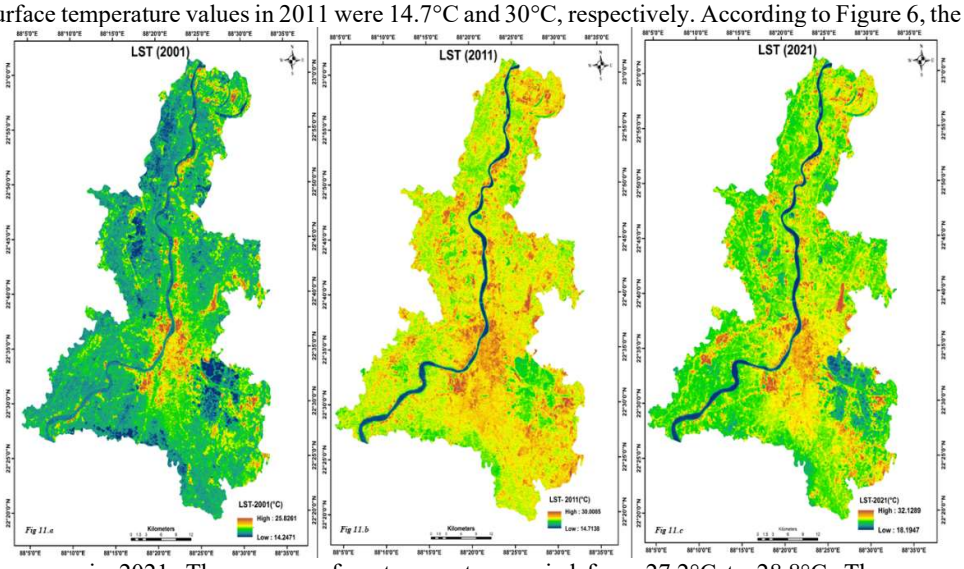

temperature zone in 2021, The mean surface temperature varied from 27.2°C to 28.8°C. The mean surface temperature in the mild zone ranged between 28.8°C and 30.4°C. The middle portion of the research area had the highest recorded temperature (30.4°C–32°C). In 2021, the surface temperature ranged from a minimum of 27.2°C to a maximum of 32°C.

Fig. 6 Areal differentiation in LST of KMA area from 2001 to 2021**3.4 Changes in MNDWI (2001-2021)**
Figure 7 shows an inverse correlation observed between MNDWI and LST. The relationship is negative because the LST values are falling while the MNDWI values are rising. Since it represents values with water pixels, the study uses the positive value of MNDWI above 0. The association between MNDWI and LST has R^2 values over -0.1, which indicates a strong connection. The relationship is negative because the LST values fall as the MNDWI values rise. Due to a reduction in the quantity of LULC in aquatic bodies, the mean LST increased during the research. The region's local climate is significantly influenced by the water bodies there. Between 2001 and 2011, the water body shrank as the LST rose. Since the typical values are below 25 °C, the water bodies have the most significant impact on LST. The MNDWI and LST have a negative association; in 2021, there was a modest correlation coefficient of -0.12, whereas in 2001, a more robust correlation coefficient of -0.49 was observed. The MNDWI pixel values surrounding the samples in KMC were much lower in 2021 due to the previous year's lack of rainfall.

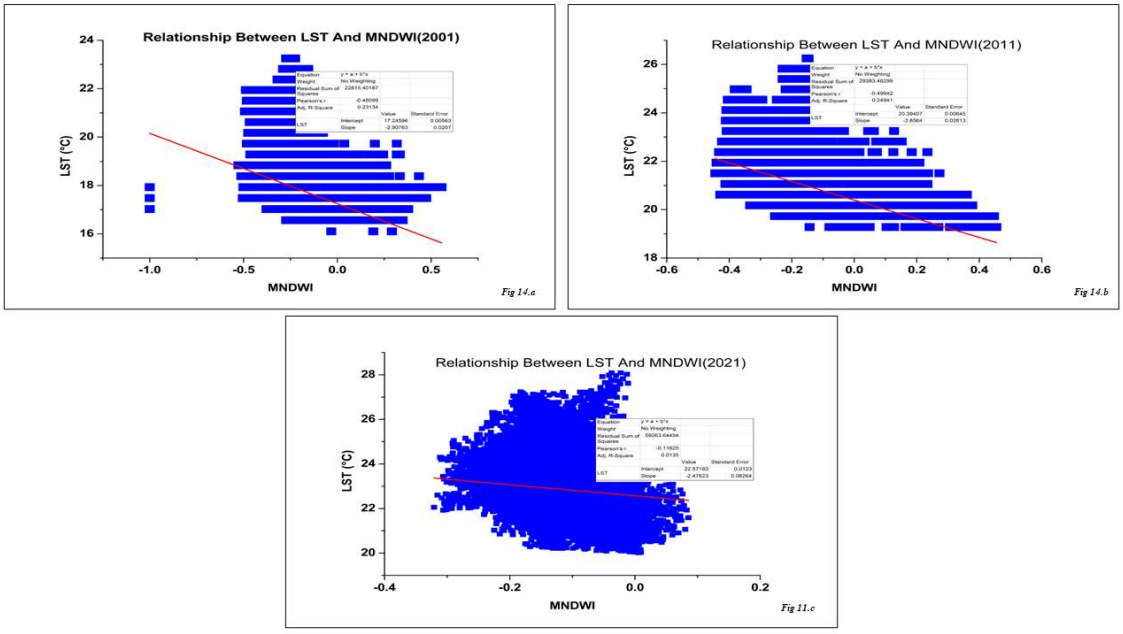

Fig. 7 Differentiation of MNDWI with LST in KMA area

3.5 Changes in NDBI (2001-2021)
The positive NDBI values over 0 are used for the study as they primarily reflect the built-up area. After investigating their interactions, a clear link between NDBI and LST was identified (Fig 8). According to the NDBI results, the built-up regions exhibited the highest surface temperature. So, it was expected that urbanization or built-up regions would result in notable differences in surface temperature. Figure 15 demonstrates a remarkable positive correlation between the NDBI and LST. For all of the years of analysis throughout the research period, the correlation between NDBI and LST exhibits a robust association, as evidenced by R^2 values exceeding 0.60. Due to the growing built-up area throughout the research period, the mean LST rises. The graph demonstrates that when the LST climbed between 2001 and 2021, the built-up area expanded dramatically.

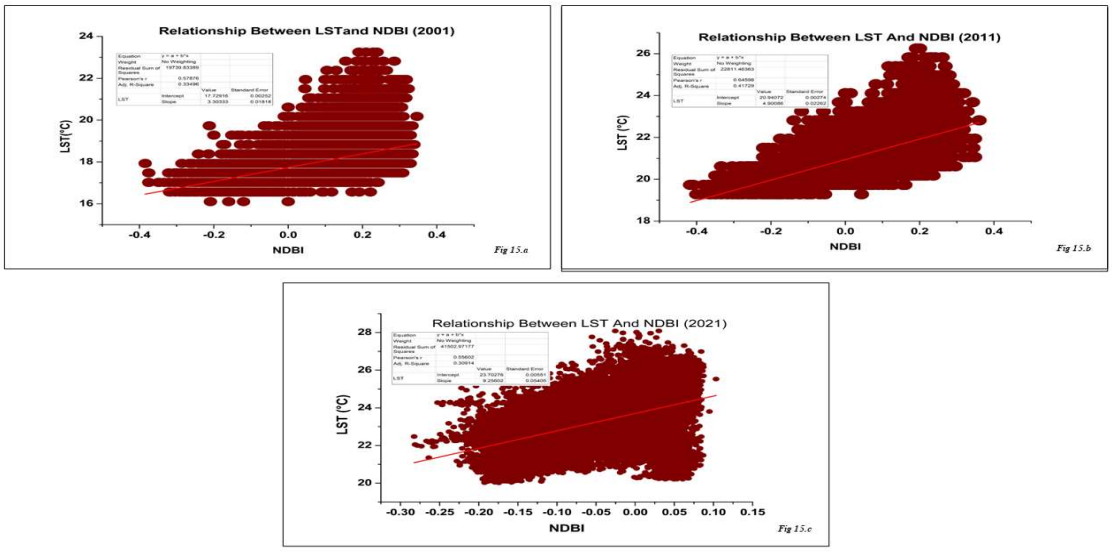

Fig. 8 Differentiation of NDBI with LST in KMA area

3.6 Changes in UNL (2001-2021)

UNL is mainly seen in urban areas that are densely populated and have many houses clustered. In other words, if the amount of LST and NDBI increases, the amount of UNL increases. We have observed the past and present conditions of UNL by combining the luminous value or DN value quantities from the UNL survey on the KMA region through their analysis. Observation of the 2001 satellite image shows (Fig 9) that the maximum luminous value according to UNL was 63, and the minimum UNL value was 0. The main central part of the KMA region, i.e. Kolkata, Howrah and a large area of North 24 Parganas, had a luminous value of 63. If we start along the Hooghly River towards the north of the KMA area, it will be seen that the amount of luminous value decreases gradually. Still, the value of UNL in the riverside area is a little higher than in other areas. Again, the luminous value is between 53 and 60 in the south, southeast and southwest regions, namely Budgebudge, Sonarpur, and Baruipur. As Dumdum, Salt Lake, and Rajarhat are swampier, the luminous value is between 35 and 45, which proves the sparseness of houses and population in that area. Similarly, in some parts of Barrackpore, Barasat, and west in Konnagar, Hindmotor, Rishra, and Chandannagar, the luminous value is between 24 and 30 due to high wetlands and sparse population.

According to the satellite image in 2011 (Fig 10), the luminous value ranged from 6 to 63. Between 2001 and 2011, as the LULC changed, the population and number of houses increased, and so did the amount of LST. In the central part of the KMA region, i.e. Kolkata, Howrah and North 24 Parganas cities, including Kolkata, the luminous value is between 60 and 63. The luminous value is between 45 and 60 in Sonarpur, Baruipur, Budgebudge, etc., in the south, southeast and southwest. The luminous value ranges from 20 to 30 for population density in East Kolkata Wetland areas. The luminous value ranges from 55 to 60 along the Hooghly River northward from Chandannagar, Kalyani, to Barrackpore or Sodpur. Urban construction with an increasing population is considered one of the reasons for this. The luminous value is between 15 and 19 due to wetlands in the western part of Konnagar from Chandannagar and the swampy area from Kalyani to Bhatpara and Barrackpore to Barasat.

Between 2011 and 2021 (Fig 11), due to excessive population growth, urban construction increased, and the luminous value ranged from 0.83 to 103.55, according to satellite images. The amount of luminous value is between 91 and 103 along various regions of North 24 Parganas and Howrah adjacent to Kolkata, including Kolkata. The luminous value has remained limited to 81 to 90 across Sonarpur, Baruipur, and the south, southeast, and southwest. From Chandannagar and Kalyani in the north to Rishara, Hindmotor and Barrackpore along industrial areas, the luminous value ranged from 85 to 98. The population and the amount of urban construction here are very high for the presence of various means of living. Salt Lake, along East Calcutta wetlands in Rajarhat, KMA east of luminous values range from 30 to 45, indicating a sparse population in this region. Also, luminous values range from 21 to 28 along the western region of KMA from Chandannagar to Hindmotor south. Similarly, luminous values are limited to 25 to 30 along the eastern part of the KMA from Kalyani south through Barrackpore

to Barasat. Usually, due to the prevalence of wetlands, variations in the amount of luminous value can be seen in this part.

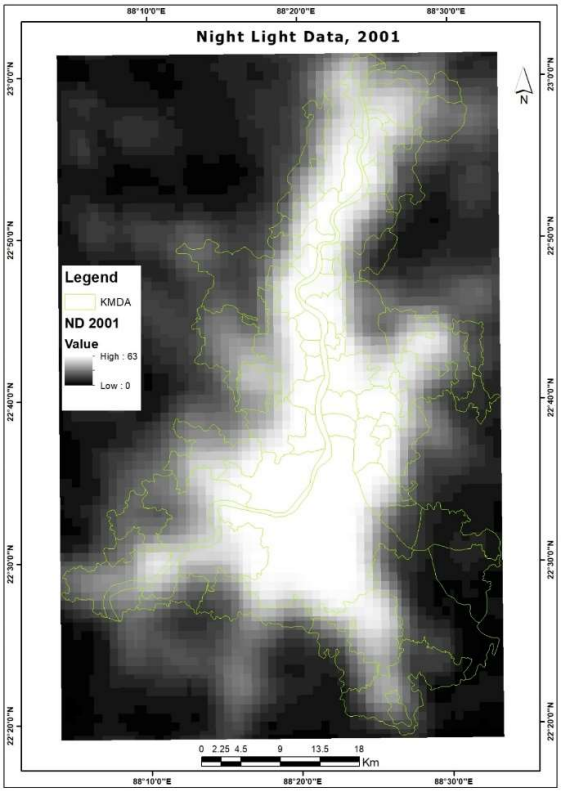

Fig. 9 UNL of 2001 in KMA area

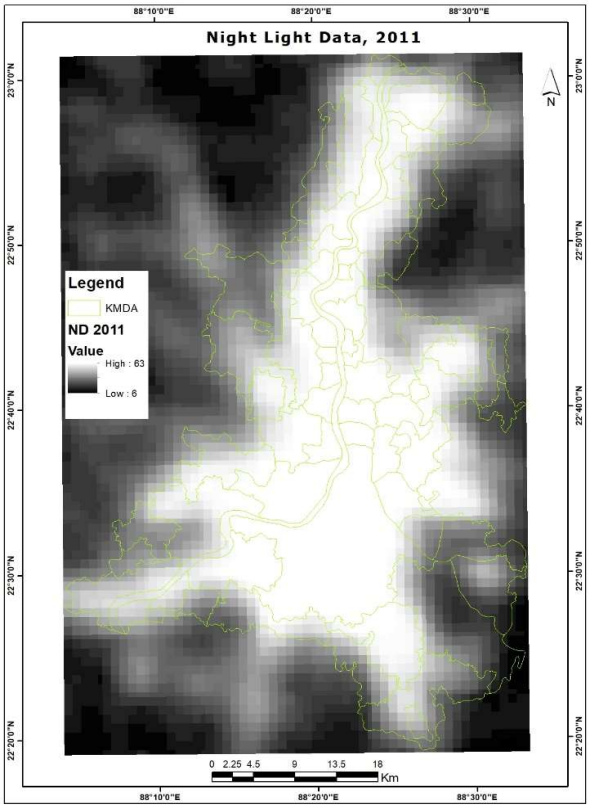

Fig. 10 UNL of 2011 in KMA area

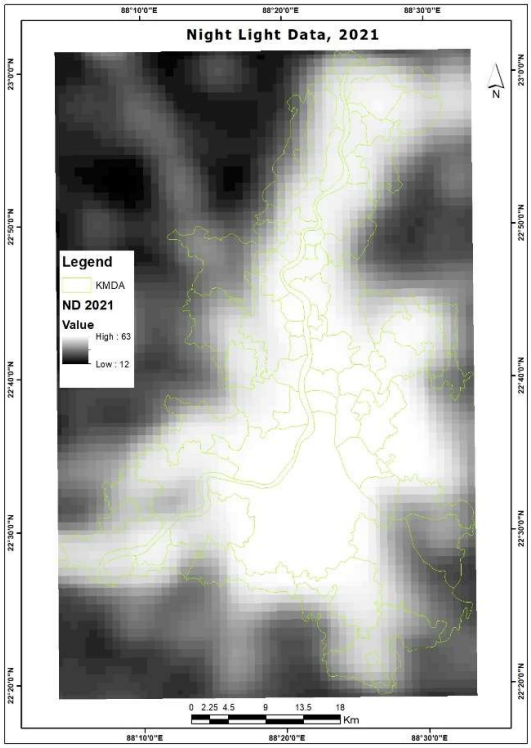

Fig. 11 UNL of 2021 in KMA area

3.7 Correlation between UNL with temporal indices (2001-2021)

In the case of UNL, its effectiveness is measured by the luminous value, and on the other hand, UNL has an essential relationship with various climatic spatial indices. NDVI and MNDWI are primarily used as a proxy for the presence of vegetation and water in an urban area, which is an essential measure of the environmental aspects of metropolitan areas. However, since UNL highlights the depth aspect of urban construction if the amount of UNL increases, the amount of NDVI or MDWI decreases, which is dangerous from an environmental point of view. On the other hand, LST and NDBI act as facilitators for the growth of urban construction. As the number of houses increases in urban areas, as LST increases, so does the amount of NDBI. On the one hand, when the luminous value of UNL increases, the value of LST and NDBI increases. From 2001 to 2021, the luminous value of UNL rose gradually in the KMA region, while the value of LST and NDBI gradually increased, but the value of NDVI and MNDWI decreased. The correlation coefficient based on decade shows the proportional relationship between the amount of luminous value of UNL and the amount of different spatial indices.

Since 2001, the value of LST has continuously increased, indicative of the increase in urban construction. According to LULC along the KMA region, urban construction has increased significantly from 2001 to 2021. If urban construction increases, the light luminance value will increase at night, significantly increasing the luminous value of UNL (Fig 12). Based on 2001 and 2011, the value of LST increased with the increase of luminous value, and the R^2 value was 0.977 and 0.975, respectively. Again, in 2021, the LST increased significantly with the luminous value, and the R^2 value was 0.989.

Since 2001, the value of NDBI has increased significantly with the increase in urban construction, and the luminous value of UNL has also increased considerably. As with LST, the increase in urban construction through NDBI has significantly increased night brightness (Fig 13). Based on 2001 and 2011, the value of LST increased with the rise of luminous value, and the R^2 value was 0.925 and 0.982, respectively. Again, in 2021, the LST increased greatly with the luminous value, and the R^2 value was 0.992.

With continuous urban expansion since 2001, green forests and wetlands have decreased significantly. People cut the green forest, buried the wetlands for their needs, and made urban constructions, which greatly disturbed the balance of the environment. Compared with the luminous value of UNL, the value of NDVI and MNDWI has decreased significantly based on a decade with the increase. From 2001 to 2021, the amount of green vegetation and wetlands in the KMA region significantly reduced decade by decade, developing a proportional relationship

with Urban Construction and UNL. Based on 2001 and 2011, the value of NDVI decreased with the increase of luminous value and R^2 value, which were 0.884 and 0.954, respectively (Fig 14). Again, in 2021, the NDVI slightly reduced with the luminous value, and the R^2 value was 0.937. From this, it can be assumed that after 2011, people increased the amount of tree planting by becoming aware of the environment. Based on 2001 and 2011, it can be seen that the value of MNDWI decreases with the increase of luminous value and R^2 value is 0.969 and 0.898, respectively (Fig 15). Again, in 2021, the MNDWI slightly reduced with the luminous value and R^2 value amounting to 0.859. From this, it can be assumed that after 2001, people became aware of the environment and increased their work on wetland conservation and creating new wetlands.

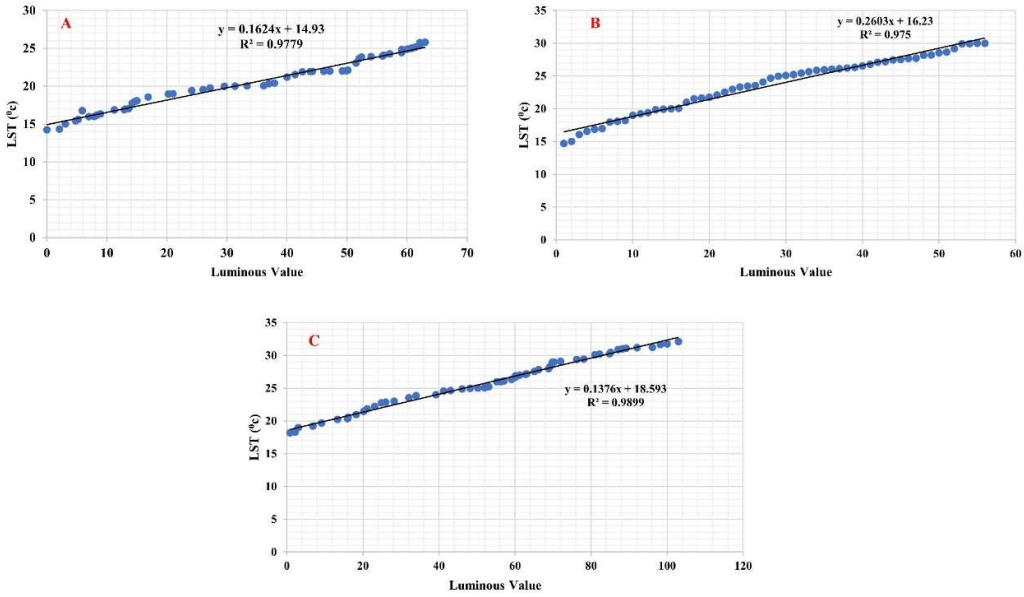

Fig. 12 Relation between LST and luminous value of UNL on A. 2001, B. 2011, C. 2021

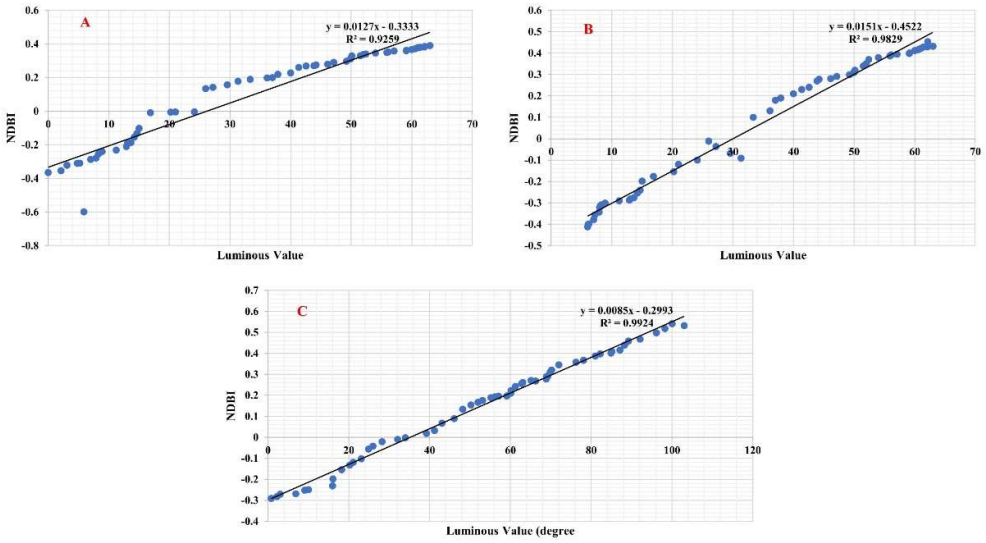

Fig. 13 Relation between NDBI and luminous value of UNL on A. 2001, B. 2011, C. 2021

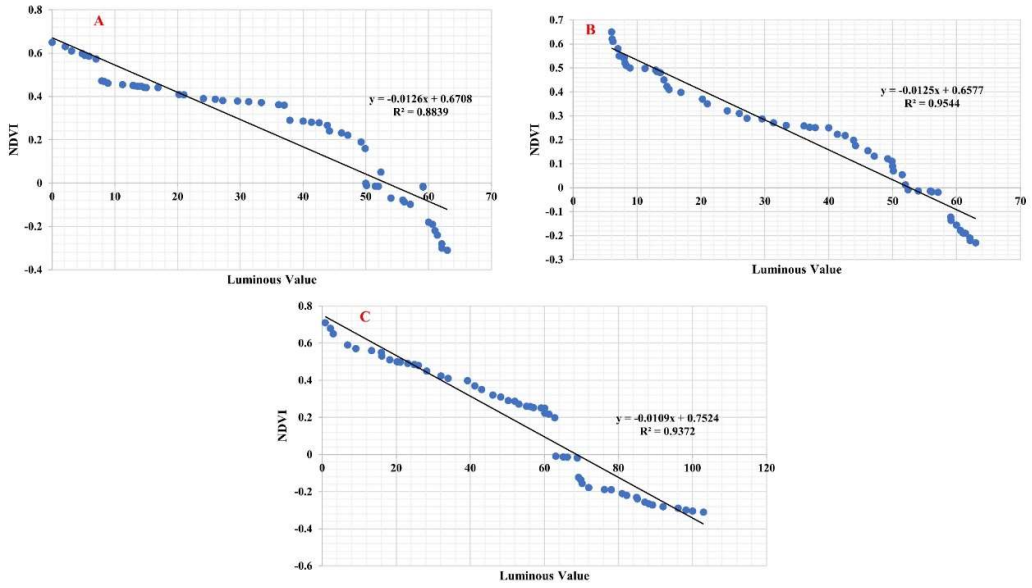

Fig. 14 Relation between NDVI and luminous value of UNL on A. 2001, B. 2011, C. 2021

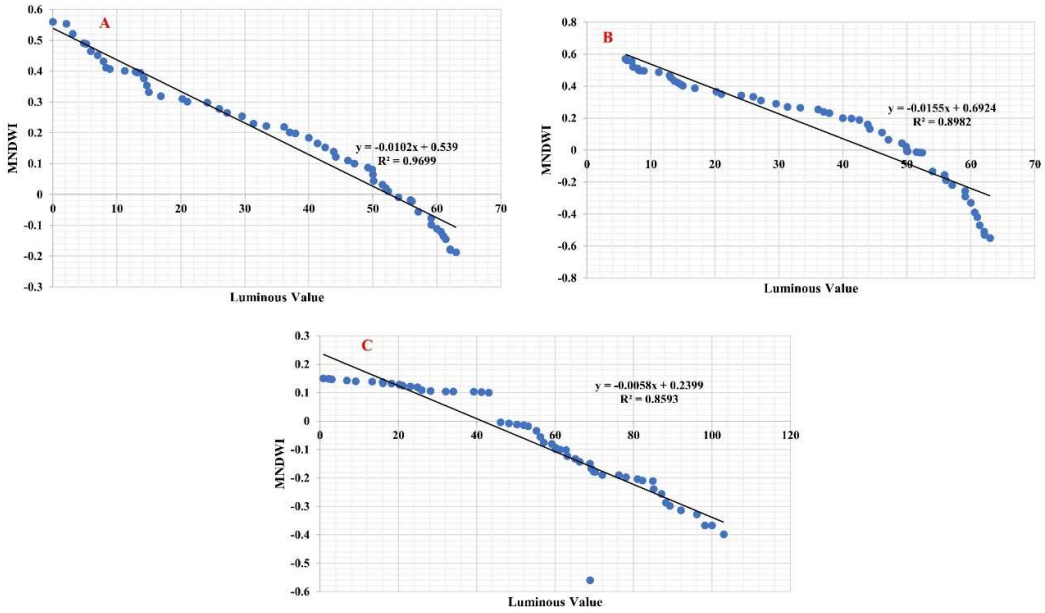

Fig. 15 Relation between NDVI and luminous value of UNL on A. 2001, B. 2011, C. 2021

4 Conclusion and recommendations

If the amount of urban construction increases in any area, the urban area will expand, and the number of houses will increase. Due to the urban area, there will be an electrification system, and the night darkness will be suppressed, and the brightness will increase. This brightness is captured through satellite images at night, and the amount of luminous value of UNL obtained from satellite images is considered evidence of urban expansion. In the three long decades from 2021 to 2021, the quality of life in the KMA region has changed with an increase in urban construction and, on the other hand, a decrease in the number of forests and wetlands. Conversely, as the rise in urban construction has degraded the quality of the environment, UNL's use of satellite images of nighttime brightness has emerged as evidence of urban expansion. The present article discusses the acceptability of using UNL as evidence of urban expansion in the KMA region. It validates this by comparing UNL with other spatial evidence of urban expansion (such as LST, NDVI, NDBI, and MNDWI). According to the modified LULC from 2001 to 2021, the built-up area in the KMA region increased by 12.55%, and the forest and vegetation decreased by 4.38%. However, people have been able to increase the number of wetlands only by 0.96% for their own needs.

According to UNL, it can be seen that from 2001 to 2021, the luminous value of Kolkata, North and South 24 Parganas near Kolkata and Howrah is significantly higher. Evidence shows that LST and NDBI are high, and MNDWI and NDVI are low in the same regions. Again, the Salt Lake in the east of the KMA region, the wetland area of Rajarhat, some parts of Barasat from Kalyani to Barakpur, the Sonarpur-Baruipur region in the south and the outskirts from Chandannagar to Konnanagar in the west have low luminous values. At the same time, LST and NDBI are low, and MNDWI and NDVI are high in all these regions. Above all, the luminous value of UNL is proportional to LST and NDBI and disproportional to MNDWI and NDVI.

Plantation programs are needed in a well-planned way to increase the amount of greenary. Greening alone will reduce the amount of LST and increase the amount of NDVI. Above all, the KMA region will be freed from the curse of UHI. However, comparing the LULC of 2011 with 2021 shows that the amount of vegetative land and wetlands in this region has increased slightly. However, humans have planned to increase the amount of vegetative land and wetlands by creating central parks, eco-parks, and fish ponds. However, in this case, the profit has been in the Salt Lake region, and it is expected that the quality of greening will shortly increase in this region through the formulation of various government plans and policies.

References

Artis, D.A., & Carnahan, W.H. (1982). Survey of emissivity variability in thermography of urban areas. *Remote Sens Environ, 12 (4)*, 313–329.

Asgher, M.S., Sharma, S., Singh, R., & Singh, D. (2021). Assessing human interactions and sustainability of Wetlands in Jammu, India using Geospatial technique. *Model. Earth Syst. Environ., 7*, 2793–2807.

Bagan, H., Borjigin, H., & Yamagata, Y. (2019). Assessing nighttime lights for mapping the urban areas of 50 cities across the globe. *EPB: Urban Analytics and City Science, 46(6)*, 1097-1114.

Bera, B., Shit, P.K., Saha, S., & Bhattacharjee, S. (2021). Exploratory analysis of cooling effect of urban wetlands on Kolkata metropolitan city region, eastern India. *Current Research in Environmental Sustainability, 3*.

Bhandari, L., & Roychowdhury, K. (2011). Night Lights and Economic Activity in India: A study using DMSP-OLS night time images. *Proceedings of the Asia-Pacific Advanced Network,32*, 218-236.

Cheon, X., & Kim, J. (2020). Quantifying the influence of urban sources on night light emissions. *Landscape and urban planning, 204*, 103936.

Dasgupta, S., Asvani, K., Gosain, K., Rao, S., Roy, S., & Sarraf, M. (2013). A megacity in a changing climate: the case of Kolkata. *Clim Chang, 116*, 747–766.

Defries, R. S., Bounoua, L., & Collatz, G. J. (2002). Human modification of the landscape and surface climate in the next fifty years. *Global Change Biology, 8(5)*, 438–458.

Duque, J.C., Lozano-Gracia, N., Patino, J.E., Restrepo, P., & Velasquez, W.A. (2019). Spatiotemporal dynamics of urban growth in Latin American cities: An analysis using nighttime light imagery. *Landsc. Urban Plan., 191*, 103640.

Fitrahanjani, C., Prasetya, T.A.E., & Indawati, R. (2021). A statistical method for analysing temperature increase from remote sensing data with application to Spitsbergen Island. *Model. Earth Syst. Environ., 7*, 561–569.

Gilbert, K.M., & Shi, Y. (2023). Nighttime Lights and Urban Expansion: Illuminating the Correlation between Built-Up Areas of Lagos City and Changes in Climate Parameters. *Buildings, 13*, 2999.

Gupta, N., Mathew, A., & Khandelwal, S. (2019). Analysis of cooling effect of water bodies on land surface temperature in nearby region: A case study of Ahmedabad and Chandigarh cities in India. *The Egyptian Journal of Remote Sensing and Space Sciences, 22*, 81-93.

Hu, T., Liu, J., Zheng, G., Li, Y., & Xie, B. (2018). Quantitative assessment of urban wetland dynamics using high spatial resolution satellite imagery between 2000 and 2013. *Sci Rep, 8*, 7409.

Jain, S., Roy, S.B., Panda, J., Rath, S.S. (2020). Modeling of land-use and land-cover change impact on summertime near-surface temperature variability over the Delhi–Mumbai Industrial Corridor. *Model. Earth Syst. Environ., 7*, 1309–1319.

Jia, D., Kaishan, S., & Baohua, Y. (2019). Impact of the Zhalong Wetland on Neighboring Land Surface Temperature Based on Remote Sensing and GIS. *Chin. Geogr. Sci., 29*, 798–808.

Katabaro, J.M., Yan, Y., Hu, T., Yu, Q. & Cheng, X. (2022). A review of the effect of artificial light at night in urban areas on the ecosystem level and remedial measures. *Frontiers in public health, 10*, 969945.

Levin, N., Kyba, C.C., Zhang, Q., de Miguel, A.S., Román, M.O., Li, X., Portnov, B.A., Molthan, A.L., Jechow,

A. Miller, & S.D., et al. (2020). Remote sensing of night lights: A review and an outlook for the future. *Remote Sens. Environ., 237*, 111443.
Li, X., & Zhou, Y. (2017). Urban mapping using DMSP/OLS stable night-time light: a review. *International Journal of Remote Sensing, 38*, 6030-46.
Li, X., Song, Y., Liu, H., & Hou, X. (2023). Extraction of Urban Built-Up Areas Using Nighttime Light (NTL) and Multi-Source Data: A Case Study in Dalian City, China. *Land, 12*, 495.
Liao, YA., Garcia-Mondragon, L., & Konac, D. et al. (2023). Nighttime lights, urban features, household poverty, depression, and obesity. *Curr Psychol, 42*, 15453–15464.
Liu, L., & Zhang, Y. (2011). Urban heat island analysis using the Landsat TM data and Aster data: A case study in Hongkong. *Remote Sens., 3*, 1535-1552.
Lunetta, R.S., Iiames, J., Knight, J., Congalton, R.G., & Mace, T.H. (2001). An assessment of reference data variability using a ‘‘virtual field reference database’’. *Photogramm. Eng. Remote Sens., 63*, 707–715.
Ma, T., Zhou, C., Pei, T., Haynie, S. & Fan, J. (2012). Quantitative estimation of urbanization dynamics using time series of DMSP/OLS nighttime light data: A comparative case study from China's cities. *Remote Sensing of Environment, 124*, 99–107.
Ma, Z., & Redmond, R.L. (1995). Tau coefficients for accuracy assessment of classification of remote sensing data. *Photogramm. Eng. Remote Sens., 61*, 435–439.
Monserud, R.A., & Leemans, R. (1992). Comparing global vegetation maps with the Kappa statistic. *Ecol. Model., 62*, 275e293.
Neteler, M. (2010). Estimating daily land surface temperatures in mountainous environments by reconstructed MODIS LST data. *Remote Sens., 2*, 333–351.
Nieuwolt, S. (1966). The Urban Microclimate of Singapore. *J. Trop. Geogr., 22*, 30–37.
Pramanik, S., & Punia, M. (2019). Assessment of green space cooling effects in the dense urban landscape: a case study of Delhi, India. *Model. Earth Syst. Environ., 5*, 867–884.
Qin, Z., Karnieli, A., & Berliner, P. (2001). A mono-window algorithm for retrieving land surface temperature from Landsat TM data and its application to the Israel-Egypt border region. *Int. J. Remote Sens., 22*, 3719–3746.
Rehman, S., Honap, V., & Siddiqui, A. et al. (2021). Spatio-Temporal Variations in Night Lights, Economy and Night Light Emissions in States of India. *J Indian Soc Remote Sens, 49*, 2933–2943.
Roy, D., Lees, M., Palavalli, B., Pfeffer, K., & Sloot, M. (2014). The emergence of slums: a contemporary view on simulation models. *Environ Model Softw, 59*, 76–90.
Satheendran, S.S., Chandran, S.S., & Mathew, J.C. (2022). The Evolution of Lighting in South-West India from Night-Time Lights: 2012–2020. *Spat. Inf. Res., 30(2)*, 261–277.
Snyder, W.C., Wan, Z., Zhang, Y., & Feng, Y.Z. (1998). Classification-based emissivity for land surface temperature measurement from space. *Int. J. Remote Sens., 19 (14)*, 2753–2774.
Stemn, E., & Kumi-Boateng, B. (2020). Modelling of land surface temperature changes as a determinant of urban heat island and risk of heat-related conditions in the Wassa West Mining Area of Ghana. *Model. Earth Syst. Environ., 6*, 1727–1740.
Townshend, J.R., & Justice, C.O. (1986). Analysis of the dynamics of African vegetation using the normalized difference vegetation index. *Int. J. Remote Sens., 7 (11)*, 1435–1445.
Verma, P., Raghubanshi, A., Srivastava, P.K., & Raghubanshi, A.S. (2020). Appraisal of kappa-based metrics and disagreement indices of accuracy assessment for parametric and nonparametric techniques used in LULC classification and change detection. *Model. Earth Syst. Environ., 6*, 1045–1059.
Weng, Q. (2001). A remote sensing-GIS evaluation of urban expansion and its impact on surface temperature in the Zhujiang Delta, China. *Int. J. Remote Sens., 22*, 1999–2014.
Xin, A. (2023). Correlation between surface temperature and population density in Xiong’an New Area based on nightlight remote sensing and Landsat8 data. *Highlights Sci. Eng. Technol., 59*, 29–36.
Yi, K., Tani, H., Li, Q., Zhang, J., Guo, M., Bao, Y., & Li, J. (2014). Mapping and evaluating the urbanization process in northeast China using DMSP/OLS nighttime light data. *Sensors, 14(2)*, 3207–3226.
Zha, Y., Gao, J., Ni, S. (2003). Use of normalized difference built-up index in automatically mapping urban areas from TM imagery. Int. J. Remote Sens., 24(3), 583–594.
Zhao, M., Cheng, W., Zhou, C., Li, M., Huang, K., & Wang, N. (2018). Assessing spatiotemporal characteristics of urbanization dynamics in Southeast Asia using time series of DMSP/OLS night-time light data. *Remote*

Sensing, 10(1), 47.
Zheng, M., Huang, W., & Xu, G. et al. (2023). Spatial gradients of urban land density and nighttime light intensity in 30 global megacities. *Humanit Soc Sci Commun, 10*, 404.
Zheng, Q., Seto, K.C., Zhou, Y., You, S., & Weng, Q. (2023). Nighttime light remote sensing for urban applications: Progress, challenges,and prospects. *ISPRS J. Photogramm. Remote Sens., 202*, 125–141.
Zhou, Q., Robson, M., & Pilesjo, P. (1998). On the ground estimation of vegetation cover in Australian rangelands. *Int. J. Remote Sens., 9*, 1815–1820.